Supplementary information

Outstanding anti-corrosion performance in Nd–Fe–B permanent magnet by constructing a hydrophobic triplex surface coating

Wang Chen,[a] Jiaying Jin,[a,*] Junyao Yu,[a] Liang Zhou,[a] Baixing Peng,[a] Song Fu,[b] Xiaolian Liu,[b] Guohua Bai,[b] and Mi Yan[a,*]

[a]*School of Materials Science and Engineering, State Key Laboratory of Silicon Materials, Key Laboratory of Novel Materials for Information Technology of Zhejiang Province, Zhejiang University, Hangzhou 310027, China*

[b]*Institute of Advanced Magnetic Materials, College of Materials and Environmental Engineering, Hangzhou Dianzi University, Hangzhou 310012, China*

[*]*Corresponding authors*. jinjy@zju.edu.cn (J. Jin), mse_yanmi@zju.edu.cn (M. Yan).

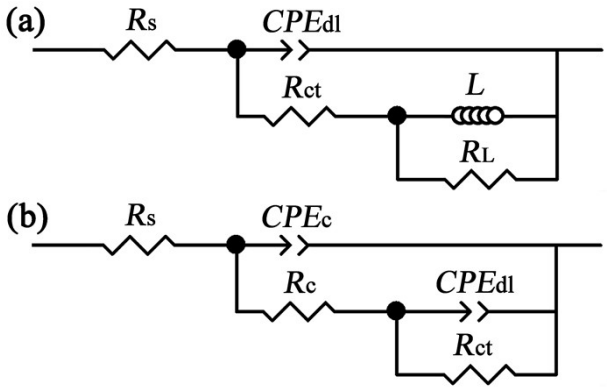

Fig. S1. Electrochemical equivalent circuit for (a) pristine and (b) oxidized Nd–Fe–B magnets in the impedance measurement. R_s is the solution resistance, R_{ct} is the charge transfer resistance, R_c is the film resistance, and R_L is the inductive reactance. CPE_{dl} and CPE_c reflect the double-layer capacitance and the film capacitance, respectively.

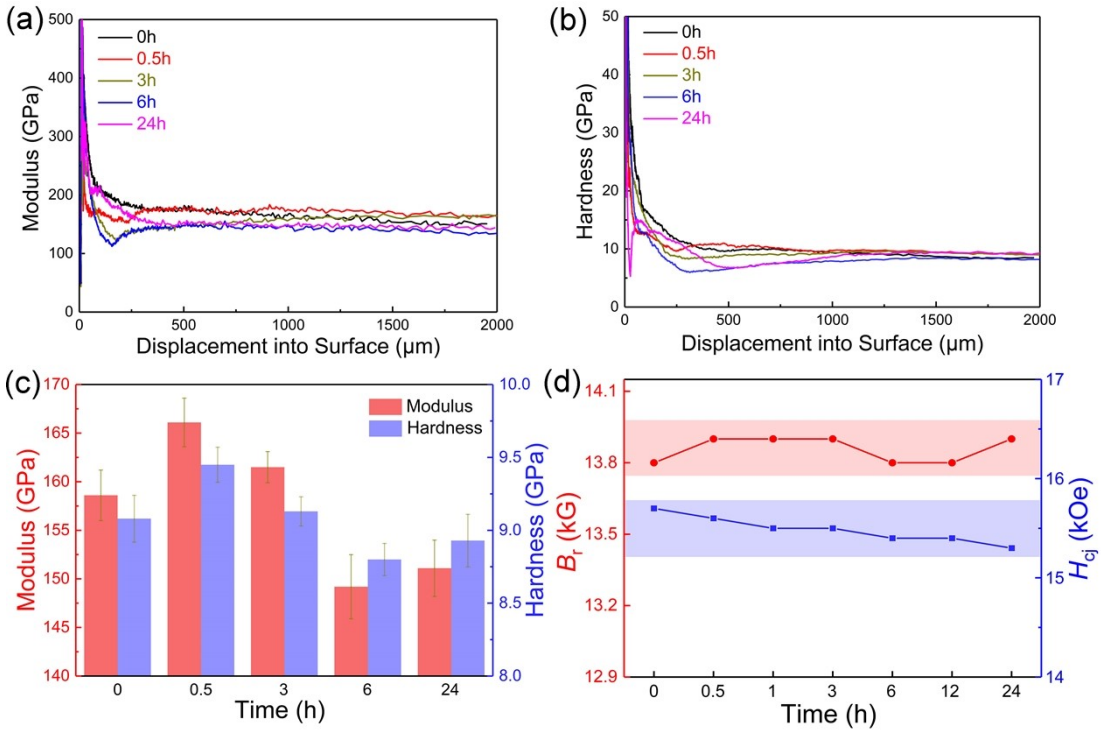

Fig. S2. Mechanical and magnetic properties of the pristine and oxidized Nd–Fe–B magnets. (a) Modulus curves, (b) hardness curves, and (c) derived mechanical values. d) Remanence B_r (red) and coercivity H_{cj} (blue) variations as a function of oxidation time.

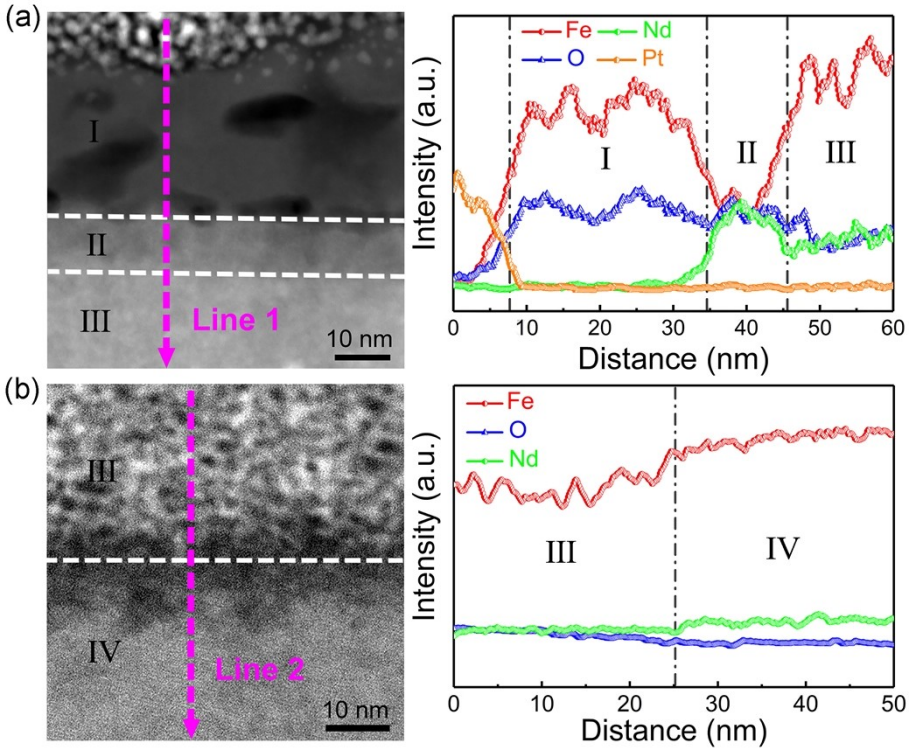

Fig. S3. HAADF-STEM image and corresponding elemental scan profiles of (a) Line 1 recorded from region A, and (b) Line 2 recorded from region B in **Fig. 5**a.

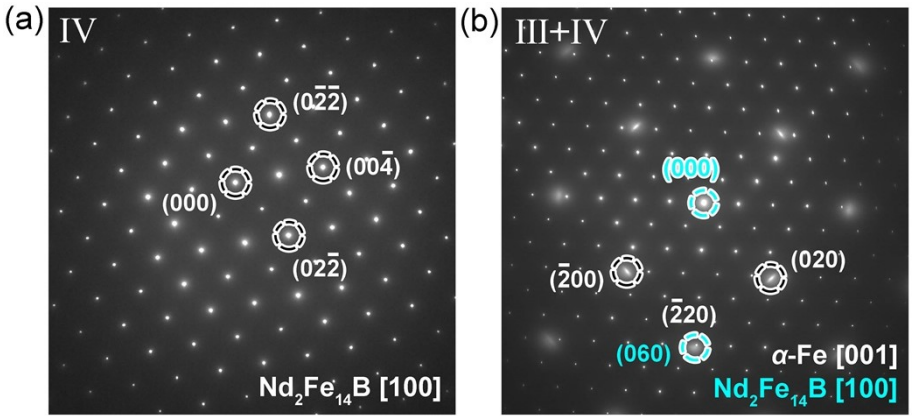

Fig. S4. Crystallographic orientation relationship between zone III and zone IV taken from **Fig. 5**. (a) SAED pattern of $Nd_2Fe_{14}B$ grain in zone IV along the [100] axis. (b) SAED pattern of the III/IV interface region, demonstrating the Burgers orientation relationship of $[001]_{\alpha\text{-Fe}}//[100]_{\text{Nd2Fe14B}}$ and $(\bar{2}20)_{\alpha\text{-Fe}}//(060)_{\text{Nd2Fe14B}}$.

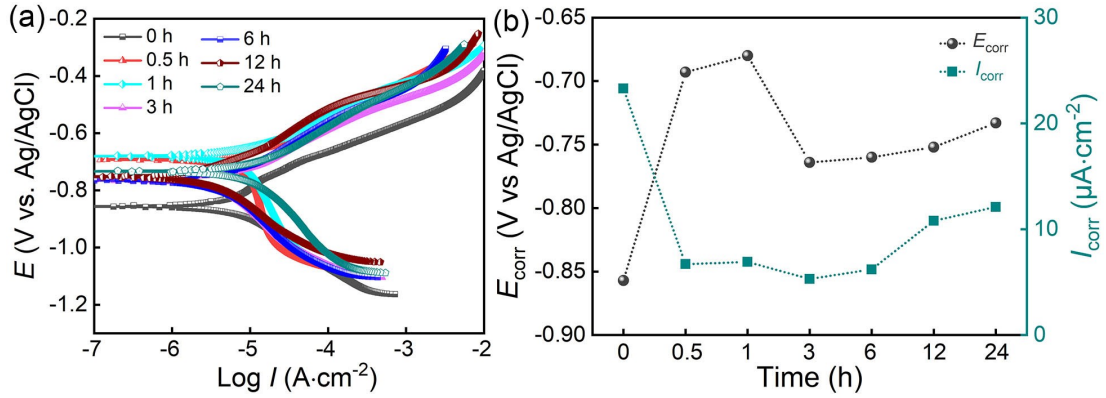

Fig. S5. Anti-corrosion performance of proof-of-principle Dy50 Nd–Dy–Fe–B magnet with a nominal composition of $[(Pr_{20}Nd_{80})_{0.5}Dy_{0.5}]_{31.0}Fe_{bal}M_{1.25}B_{1.0}$ (M= Co, Al, Cu, Ga, Zr, wt.%). (a) Electrochemical polarization curves of the pristine and oxidized Dy50 magnets in 3.5 wt.% NaCl solution, (b) derived corrosion potential (E_{corr}) and corrosion current density (I_{corr}).

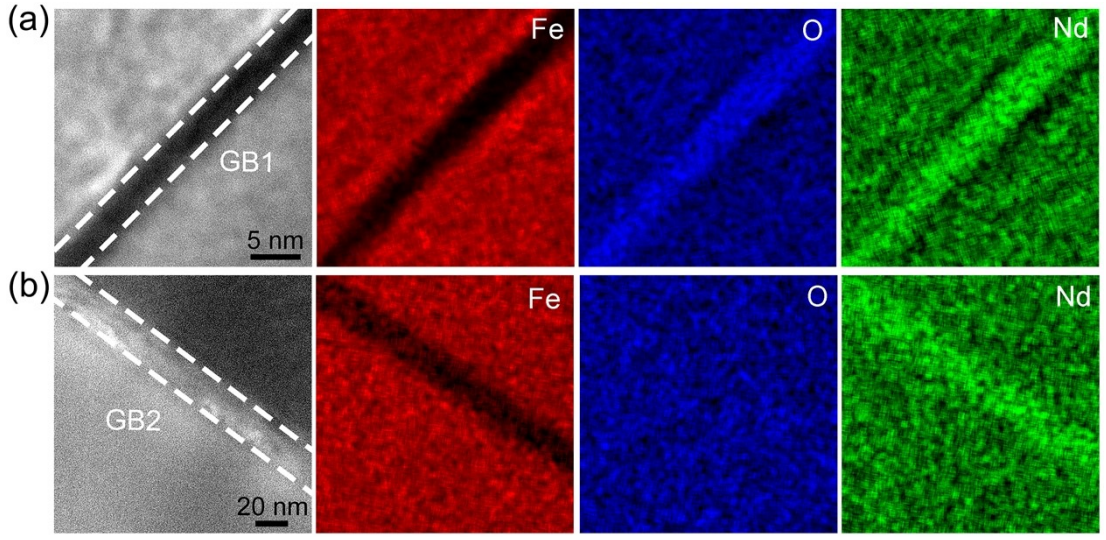

Fig. S6. HAADF-STEM image and corresponding STEM-EDS mappings for (a) GB1 and (b) GB2 obtained from zone III and zone IV in **Fig. 6**a, respectively.

Table S1. Electrochemical parameters of the pristine and oxidized Nd–Fe–B magnets in 3.5 wt.% NaCl solution.

Samples	E_{corr} (V)	I_{corr} ($\mu A \cdot cm^{-2}$)	R_s ($\Omega \cdot cm^2$)	Q_c ($F \cdot cm^{-2} \cdot s^{n-1}$)	n_c	R_c ($\Omega \cdot cm^2$)	Q_{dl} ($F \cdot cm^{-2} \cdot s^{n-1}$)	n_{dl}	R_{ct} ($\Omega \cdot cm^2$)	L ($H \cdot cm^2$)	R_L ($\Omega \cdot cm^2$)
0 h	-0.93	27.3	47.0	/	/	/	1.82×10^{-4}	0.790	1528	1645	551
0.5 h	-0.86	4.7	56.1	3.53×10^{-4}	0.757	16.3	6.23×10^{-9}	0.745	4580	/	/
1 h	-0.86	5.6	53.9	3.76×10^{-4}	0.804	23.1	1.50×10^{-11}	0.723	2885	/	/
3 h	-0.85	4.8	57.2	3.36×10^{-4}	0.797	25.0	6.40×10^{-12}	0.730	2678	/	/
6 h	-0.74	18.4	63.5	4.91×10^{-4}	0.823	65.0	7.84×10^{-11}	0.826	2577	/	/
12 h	-0.75	24.9	56.6	2.34×10^{-4}	0.751	107.6	1.03×10^{-4}	0.704	2456	/	/
24 h	-0.77	22.7	63.4	2.47×10^{-4}	0.841	395.6	1.13×10^{-4}	0.873	1682	/	/